Facies (2004) 50:327–346
DOI 10.1007/s10347-004-0019-4

ORIGINAL ARTICLE

Heiko Hüneke · Kay Krienke

Toe-of-slope deposits of a Givetian reef-rimmed platform: provenance of calcareous density-flow deposits (Rabat-Tiflet-Zone, Morocco)

Received: 2 March 2004 / Accepted: 4 May 2004 / Published online: 10 July 2004

Abstract Givetian subaqueous density-flow deposits reveal the existence of a peritidal carbonate platform in sedimentary basins preserved within the Rabat-Tiflet-Zone of Morocco. The calcareous component assemblage displays a photozoan carbonate production mode of the neritic source environments. Characteristic elements of the allochthonous faunal association are colonial tabulate corals, stromatoporoids, crinoids, bryozoans and thick-shelled brachiopods. Active growing reefs and cortoid sand shoals at the platform margin as well as periplatform carbonates at the uppermost slope settings contributed bioclastic and lithoclastic lime debris to the toe-of-slope of the carbonate apron. Bipartite cobble rudstone beds are interpreted as deposits of hyperconcentrated density flows, which cannot be maintained on very low-angle slopes for as long as more dilute flows and represent short run-out distances. Beds consisting of mostly well-organized pebbly grainstones, packstones and grainstone-wackestone couplets are deposits of surge-like concentrated flows and turbidity flows.

Keywords Morocco · Middle Devonian · Toe-of-slope deposits · Carbonate apron · Density flows · Turbidity flows · Provenance

Introduction

Silurian to Middle Devonian strata of the Rabat-Tiflet-Zone in Morocco (Fig. 1) exhibit striking similarities in their lithofacies and biofacies development, as well as their stratigraphic history, to those of the classical Prague Basin within the Tepla-Barrandian of Central Europe (Czech Republic). This is true in particular for the western parts of the Rabat-Tiflet-Zone and was mentioned early by Hollard (1967), Alberti (1969, 1970), Destombes et al. (1985) and Walliser et al. (1995b). Sedimentological and stratigraphical investigations serve as a basis for a detailed comparison between these basins and an evaluation of late Variscan strike-slip movements. This paper focuses on Givetian carbonates which are exposed south of Tiflet at the northern margin of the Moroccan Central Massif. These are subaqueous density-flow deposits which document continuing marine sedimentation, including reef growth, at least up to the middle Givetian, within the Moroccan basin. This contrasts with the succession of the Prague Basin, where the onset of siliciclastic sedimentation near the Eifelian-Givetian boundary is interpreted as a reflection of early Variscan orogenic processes (Chaloupský et al. 1995). Black shales reflecting the Kačák event and overlying coarser siliciclastics of the Robín member represent the youngest sediments within the Tepla-Barrandian which are affected by the Variscan deformation.

The documented succession is well exposed about 900 m east of the river Tiflet, to the north of the quarry road (mapsheet 1:50000, no. NI-29-XII-4c Tiflet; r 418 100, h 363 500).

H. Hüneke (✉)
Institut für Geographie und Geologie,
Universität Greifswald,
Jahn-Strasse 17a, 17487 Greifswald, Germany
e-mail: hueneke@uni-greifswald.de
Tel.: +49-3834-864567
Fax: +49-3834-864572

K. Krienke
Wolfgang-Heinze-Straße 11a, 18437 Stralsund, Germany

Geological Setting

The metamorphic northern part of the Rabat-Tiflet-Zone (Sehoul-Zone) was consolidated during the Caledonian Orogeny (Fig. 2). Dating of cleavage and metamorphism by K/Ar isotopes indicate a late Ordovician age (~ 450 Ma) for the folding phase (El Hassani 1991). The deformed Cambrian clastic sediments, several hundred metres thick, are interpreted as a deltaic succession.

The west-east trending central part of the Rabat-Tiflet-Zone (Bou-Regreg-Zone) exhibits Early Ordovician and Late Silurian to Middle Devonian strata which, in turn, are overlain disconformably by Late Devonian to Early

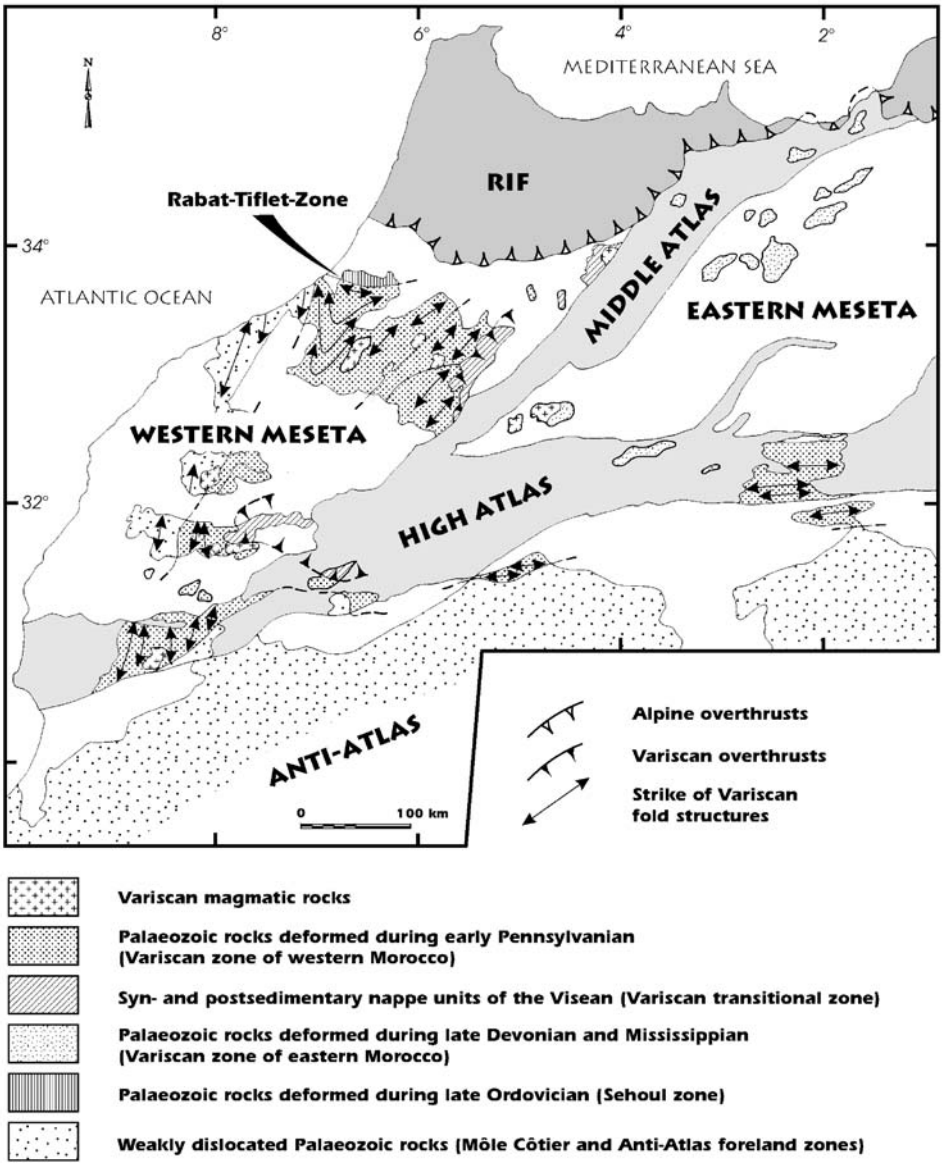

Fig. 1 Schematic tectonic map of northwest Africa (Morocco) showing the main Variscan massifs (modified from El Hassani (1991)

Carboniferous sediments of the Satour-Basin. The whole succession was deformed during the Variscan orogeny.

Early Ordovician siliciclastic strata include oolitic ferromagnesian silicates and calc-alkaline volcanic rocks. The absence of Late Ordovician and Early Silurian strata is attributed to the Caledonian deformation in the Sehoul-Zone forcing subsequent uplift of the whole area (El Hassani 1991). Late Silurian to Middle Devonian pelites and carbonate sediments reflect marine accumulation under conditions of lithospheric extension, which increased from Early Devonian times. Latest Devonian to Early Carboniferous sediments rest in part unconformably on older strata. These are conglomerates and mostly marine siliciclastic sediments which fill a small east-west trending trough (Satour-Basin). Coeval clastic sediments are also widespread in the southern part of the Rabat-Tiflet-Zone (Sidi-Bettache-Basin). As a result of the Variscan deformation the Palaeozoic sediments of the Bou Regreg Zone and the Sidi Bettache Basin were folded and were thrust over from the north by the Sehoul block. Therefore, a mylonitic shear zone separates the metamorphic Caledonian deformed zone in the north from the Variscan deformed zones in the central and southern parts of the Rabat-Tiflet-Zone (El Hassani 1991). Furthermore, tectonic deformation resulted in east-west trending faults which now bound the various blocks of Palaeozoic rocks. The locality is situated at the southern flank of the southern syncline at Tiflet (see El Hassani 1991).

The Mesozoic and Cenozoic was a time of stable platform conditions. Triassic pelites and basalts are restricted to the southeast of the area, whereas Cenozoic rocks unconformably rest on the Mesozoic peneplain.

Stratigraphy

The Tiflet section represents an early Givetian limestone succession spanning the *hemiansatus* and *timorensis*

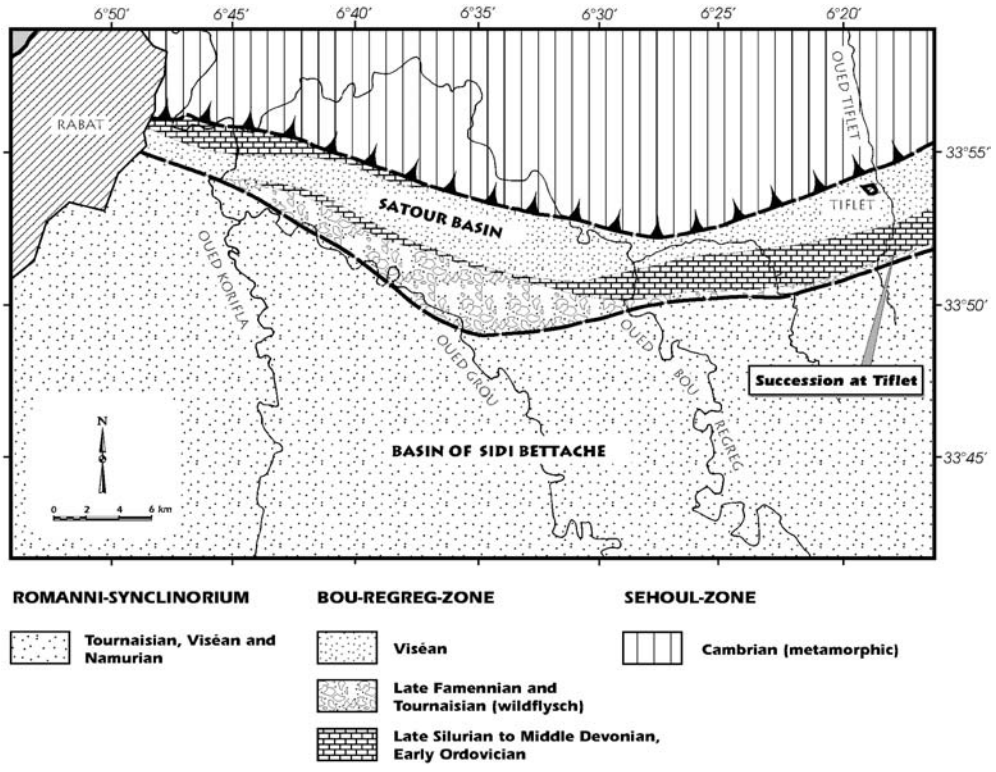

Fig. 2 General structural subdivision of the Rabat-Tiflet-Zone at the northern margin of the Moroccan Central Massif (according to El Hassani 1991)

Table 1 Distribution and number of conodont species from the section at Tiflet (early Givetian). Sample points are shown in Fig. 3 (T1 at 0.55 m, T2 at 2.20 m, T3 at 5.55 m, T4 at 5.65 m and T 18 at 27.35 m)

Conodont sample (T) -	1	2	3	4	18
Weight dissolved (kg)	6.1	4.1	2.7	3.8	6.3
Polygnathus ensensis Ziegler & Klapper 1976	1				
Polygnathus timorensis Klapper, Philip & Jackson 1970					>10
Polygnathus varcus Stauffer 1940					1
Polygnathus kluepfeli Wittekindt 1966	1				
Polygnathus linguiformis linguiformis Hinde 1879	6	4	1		>10
Polygnathus linguiformis klapperi Clausen, Leuteritz & Ziegler 1979	1	1			5
Tortodus variabilis (Bischoff & Ziegler 1957)	1				
Icriodus regularicrescens Bultynck 1970			2	1	
Icriodus obliquimarginatus Bischoff & Ziegler 1957	3	1			
Belodella resima (Philip 1965)	3				
Coelocerodontus sp. Etmington 1959	1				
Conodont standard zonation	*hemiansatus* Zone				Lower *varcus* Zone
Polygnathus zonation (Bultynck 1987)	*hemiansatus* Zone				*timorensis* Zone
Icriodus zonation (Bultynck 1987)	*obliquimarginatus Zone*				

Zones. In terms of the conodont standard zonation (Ziegler et al. 1976, Weddige 1977, Walliser et al. 1995a) the documented accumulation of density-flow deposits began during the late *hemiansatus* Zone at the latest and reached up through the Lower *varcus* Zone (Table 1). In addition, biostratigraphic dating is based on information given with the alternative *Polygnathus* and *Icriodus* zonations proposed by Bultynck (1987). A total of 10 conodont samples, each 10 kg, was collected, but only 5 samples yielded an identifiable fauna.

Conodont faunas from the base of the succession (samples T1 and T2) contain *Icriodus obliquimarginatus* which clearly indicates an early Givetian age. The species defines the base of the *obliquimarginatus* Zone in neritic areas (Bultynck 1987). However, neritic faunas are probably stratigraphic admixtures that commonly occur within sediment density-flow deposits (Krebs 1964; Junge 1997). More distinctive, *Tortodus variabilis* and *Polygnathus kluepfeli* (sample T1) point to an age covering a short period across the boundary between the *hemiansatus* Zone and the Lower *varcus* Zone (see Bultynck 1987; Weddige 1977). The occurrence of *Icriodus regularicrescens* in slightly younger beds (samples T3 and T4) is in accordance with this age interpretation for the lower part of the succession.

The occurrence of *Polygnathus timorensis* within sample T18 indicates the *varcus* Zone. Whereas a single *Polygnathus varcus* has been recovered, *P. rhenanus*, *P.*

ansatus nor other younger species have been found. Consequently, the upper part of the succession must have been deposited during early parts of the Lower *varcus* Zone (see Ziegler et al. 1976; Bultynck 1987). This interval corresponds to the *timorensis* Zone of the alternative *Polygnathus* zonation proposed by Bultynck (1987).

Facies of sediment-flow deposits

Principally, the facies description below uses the hierarchical classification of Pickering et al. (1986, 1989). Criteria are the texture of the gravelly, sandy or silty divisions of the beds, relative thickness of mud interbeds or caps, and the internal organisation of individual beds. For a detailed subfacies description, the letter code of Ghibaudo (1992) is applied (Fig. 3). The interpretation follows the nomenclature of subaqueous sedimentary density flows by Mulder and Alexander (2001), which is based on physical flow properties and grain-support mechanisms.

In order to describe the grain-size of the carbonate components, the modified Udden-Wentworth scale of Blair and McPherson (1999) is used in addition to the classification scheme of Dunham (1962) expanded by Embry and Klovan (1972). Siliciclastic components only occur in grain-sizes of fine silt and clay. Therefore, for the sake of brevity, the description of gravel- and sand-sized components always refers to carbonate components. For the description of smaller components a differentiation is made between siliciclastic and carbonate grains.

Cobble rudstones, disorganized-stratified (A2.6 → A1.1 → A2.5)

Description. This facies comprises beds that consist of clast-supported lime gravel throughout most of the bed (m), plus a thin, discontinuous cap of pebbly lime sand (s). Locally, the main gravel body is underlain by a thin basal interval of inversely graded lime sand (ig). Individual beds may reach a thickness of nearly two metres. These beds are more or less flat-based, but the outcrop dimension does not allow a thorough examination of the large-scale bed architecture. Upper surface geometry is generally irregular and undulating, with individual boulders projecting out of the bed.

(ig) Inversely graded lime sands reach a maximum thickness of 0.20 m. Packstones, grainstones and granule rudstones display a well-developed size gradation.

(m) The main gravel body typically consists of disorganized lime clasts that range from pebble to boulder grade (max. 0.6 m Ø), but cobbles are most typical. Components comprise lithoclasts and biodetritus such as bioclastic grainstones and fragments of huge coral colonies (see the section on Provenance.). The gravels are clast-supported throughout and poorly to moderately well sorted. Most of the gravel is subangular to rounded, but clast roundness is less significant, since packing fabrics vary from clast-supported to interpenetrating as a result of pressure dissolution. Generally, clasts lack a well-ordered fabric, although concentrated, elongate clasts exhibit a poorly-defined parallel alignment with bedding, or a slight imbrication. Furthermore, a crude stratification is indicated by lime sand which is the groundmass at various levels. In contrast, levels without a sandy matrix commonly show sutured clasts and diagenetically enhanced packing.

(s) The uppermost unit of stratified pebbly lime sand exhibits an alternation of pebble- and sand-rich layers. Individual layers have gradational contacts with both normal and inverse grading. Pebble-rich layers may pinch and swell and may consist of thin to very thin stringers of gravel as little as one pebble thick. Stratification may also occur on a finer scale with alternation of granule rudstones and grainstone-packstones.

Interpretation. The facies of clast-supported gravels within the main interval (m) is generally comparable to the Facies A1.1 (disorganized gravel) of Pickering et al. (1989). Examination of clast-size distribution did not result in the detection of any kind of grading. However, this is probably the result of the variable bulk density of bioclastic and/or lithoclastic lime gravels. In particular, the differential degree of cementation of the clasts at the time of redeposition may have allowed large, uncemented coral boulders to settle "out of place" at the top of the bed (see Fig. 3, metre 30.2). This feature feigns a crudely defined inverse grading that may be a coarse-tail grading or a disorganized state. A well defined inverse distribution grading is only found below the disorganized gravel interval (ig; see Fig. 3, metre 27.0) showing some relationship to Facies A2.6 (inversely graded pebbly sand) of Pickering et al. (1989). The uppermost unit of stratified pebbly lime sand (s) corresponds to Facies A2.5 (stratified pebbly sand) of Pickering et al. (1989).

Transport process. The transport mechanism of mud-poor, sandy coarse gravel of thick to very thick beds is rather poorly understood (see Ghibaudo 1992; Shanmugam 1996, 1997, 2000; Mulder and Alexander 2001). The well-developed grain-supported fabric, the low sand-content within clast interstitials and the absence of cohesive mud of the disorganized gravel division (m) suggests transport of clasts by hyperconcentrated density flows. The character of these frictional flows depends not only on the proportion of cohesive and non-cohesive particles, water content and flow velocity but also on the relative density of the fluid and particles and the particle size (Julien and Lan 1991). Coarse-grained sediment is restricted to the basal granular flow in which the particles are mainly supported by matrix and grain-to-grain interaction. The flow is primarily driven by inertia forces under conditions of high excess pore pressure (Norem et al. 1990; Inverson 1997; Marr et al. 1997; Gee et al. 1999) and hydroplaning may occur (Mohrig et al. 1998).

Depositional process. The disorganized gravel division (m) represents frictional freezing on a decreasing bottom

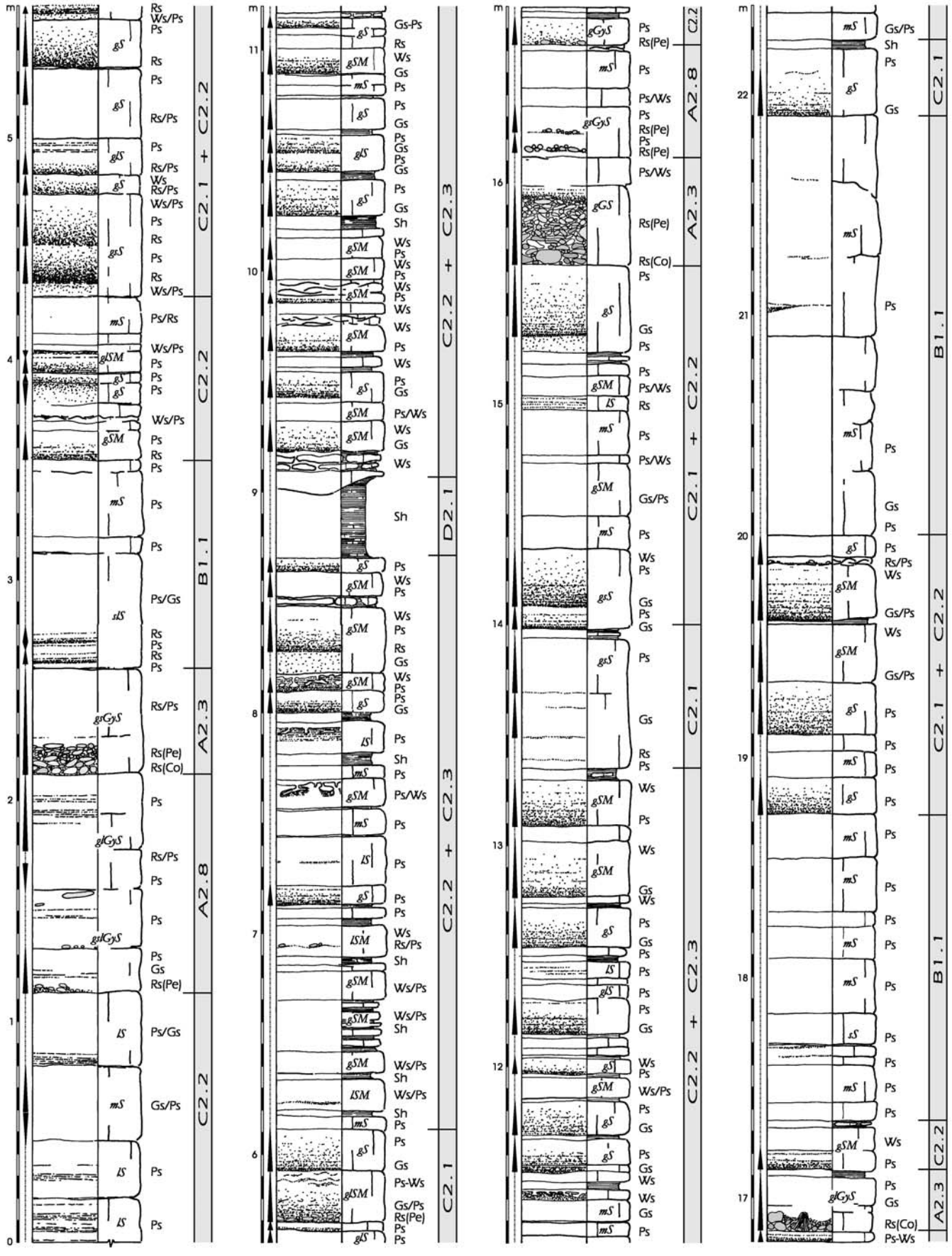

Fig. 3 Log of a representative and well exposed section of the Givetian succession south of Tiflet. *Polygnathus hemiansatus* and *timorensis* zones are recognized. The lower and upper boundaries of the lithostratigraphic unit were not exposed

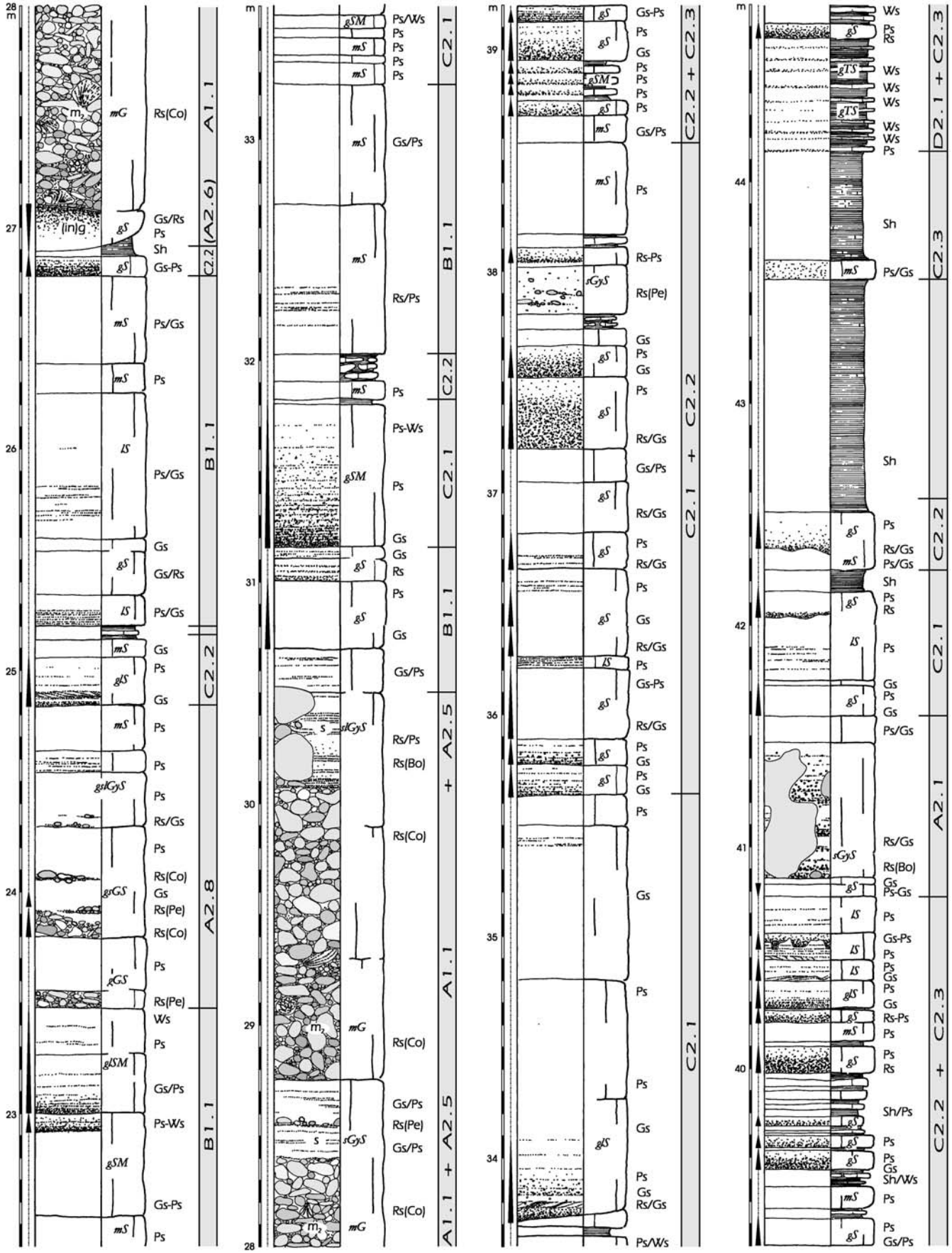

Fig. 3 (continued)

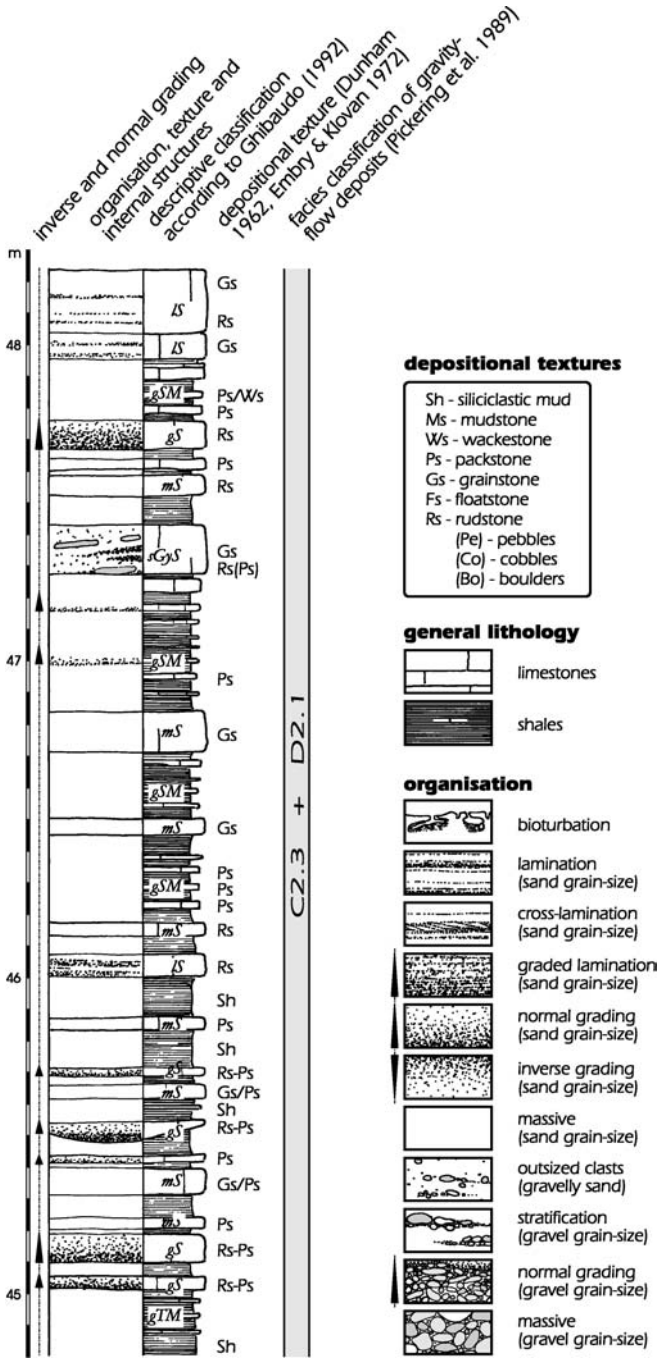

Fig. 3 (continued)

slope due to grain-to-grain interaction. Deposition proceeded by the vertical accretion of successive small-scale flow surges to the top of previous deposited layers (Major 1997). But the clasts underwent little or no traction transport after reaching the bed, probably because of relatively rapid deposition and water escape. Normal grading is not developed because suspension fall-out is unimportant (Mulder and Alexander 2001). The inversely-graded division (ig) points to rapid deposition from a traction carpet at the base of the flow (Hiscott 1994, 1995; Sohn 1997). The inverse grading is a consequence of both an upward velocity gradient within the flow and a laminar regime. The stratified pebbly sand division (s) documents deposition and reworking by the overlying associated lower concentration flow (relatively enriched in pebbles and sand) which produced a thin cap of tractional deposit. Traction and reworking may start only when water escape from the main gravel body comes to an end.

Cobble rudstones, normally graded (A2.3)

Description. Beds of this facies are couplets of clast-supported lime gravel overlain by lime sand displaying well defined grain-size grading. The facies consists of laterally continuous, parallel-sided medium to thick beds. Sole marks are not preserved.

The most obvious internal sedimentary feature is a well-defined normal grading that is commonly a distribution grading (Fig. 5C). Clast size ranges from cobble-grade at the base to sand-grade at the top with more than 50% gravel-grade material as a whole. The gravels are characterized by a high percentage of elongate clasts that show a well-defined parallel alignment with bedding. Imbrication is not typical. Frequently, the clast-supported packing texture was transformed into interpenetrating clast contacts by pressure dissolution preventing an estimation of roundness (Fig. 6D). Components comprise lithoclasts and biodetritus such as bioclastic grainstones and fragments of coral colonies (see the section below — Provenance).

Interpretation. This facies is comparable with the stratified, normally graded breccia beds illustrated by Krause and Oldershaw (1979) to exemplify intermediate-distal positions within a submarine sediment density-flow model for resedimented carbonates. The facies corresponds well to Facies A2.3 (normally graded gravel) of Pickering et al. (1989).

Transport process

True turbidity flows do not have the capability of transporting large clasts such as cobble-grade lime gravel. The presence of a distinct vertical trend in sediment size and sorting indicate transport by concentrated density flows (Mulder and Alexander 2001). A particular important particle-support mechanism is grain-to-grain interaction and less fluid turbulence. The energy exchanged by grain collisions helps to maintain them in suspension.

Mutti et al. (1999) interpret turbidite facies associations containing a substantial proportion of conglomerates and pebbly sandstones as the deposits of submarine granular flows which rapidly become bipartite flows as soon as they are accelerated and funnelled into submarines conduits. These bipartite flows include a basal, faster-moving and denser flow where turbulence is damped by high sediment concentration and a more turbulent flow above (Piper and Normark 1983; Ravenne and Beghin 1983; Norem et al. 1990;

Masson 1994). Although grain-to-grain interaction remains the main particle-support mechanism throughout the run-out of the flow, fluid turbulence acts as the dominant support mechanism near the top of the flow and at the flow head. During the downslope motion, coarser grains outdistance finer grains within the basal granular part of the flow. When the frontal part of the flow freezes, finer grains which were being transported behind overtake and step over the newly formed deposits and keep moving downcurrent.

Depositional process

By definition, the dilution of the concentrated density flow is sufficient to allow particle fall-out within the flow so that there is a significant sorting during the flow duration (Mulder and Alexander 2001). Normally graded gravels result from grain-by-grain deposition directly from the flow (Lowe 1982). Since the beds exhibit a high degree of normal distribution grading, the flows have achieved a high degree of vertical and lateral size segregation. The clasts undergo little or no traction transport after reaching the bed, because of relatively rapid deposition.

Pebbly grainstone/packstones, graded-stratified (A2.8)

Description. This facies comprises beds and successions of beds which consist of stratified, pebbly lime gravel, grading upwards into lime sand. The medium to thick beds are laterally continuous and parallel-sided. Most beds have a sharp planar base, but basal erosion and trough-shaped scour-and-fill stratification are rare. Bed contacts are diffuse where amalgamation occurs.

Successions of this facies typically show an overall coarse-tail grading from the lowest to the uppermost bed, although layers of coarser clasts are repeated upward throughout the succession, displaying well-defined stratification. In other cases, beds show coarse-tail grading in their lower parts and distribution grading in the upper parts. Clast-size ranges from pebble-grade (in some cases cobble-grade) to medium sand-grade with less than 40% gravel-grade material as a whole. However, clasts coarser than fine pebbles appear to be confined to the lower portion of the bed succession (Fig. 4B). There, an alternation of pebble- and sand-rich layers is typical, showing graded to plane-stratified and locally cross-stratified intervals. Individual strata have gradational contacts with both normal and inverse grading. Locally, pebble-rich layers may pinch and swell and split into irregular lenses and stringers. Higher up, lamination comprises faint oblique and mostly parallel multiple sets. Furthermore, distinct jumps in sediment composition and repeated inverse- to normal-graded layers are common within the vertical internal succession. As with the previous cobble rudstones facies, the beds of this facies usually lack mud caps.

Interpretation. This facies is tentatively assigned to Facies A2.8 (graded-stratified pebbly sand) of Pickering et al. (1989). Inversely graded intervals, which do not occur in clastic counterparts, probably result from a variable bulk density of the limestone clasts. Whether a generalized Lowe-like sequence is applicable (S_1 to S_3) remains unclear.

Transport process. The presence of a pronounced (but crude) normal grading, rare erosional features, bedforms and resulting sedimentary structures point to transport by concentrated density flows (Mulder and Alexander 2001). Rapid sedimentation of cobbles/pebbles (see the section above on cobble rudstones, normally graded) leaves a flow relatively enriched in fine pebbles, sand and mud (Mutti et al. 1999). Upper parts of the flows probably became more dilute and turbulent with time.

Depositional process

Normally graded gravel and coarse sand result from grain-by-grain deposition directly from the flow (Lowe 1982). At sites where the basal flow layer has a lower particle concentration, traction features can develop (Lowe 1982). Bedforms arose if flow conditions were maintained for long enough such as those described from Savoye et al. (1993) and Morris et al. (1998). Grains were transported as bedload to form horizontal, oblique and cross-stratification with common amalgamation before being buried.

Grainstone/packstones, disorganized (B1.1)

Description. This facies comprises coarse to medium lime sand beds which are more or less structureless. These beds form successions of laterally continuous, parallel-sided medium to thick beds. Sole marks were not found. Beds are locally amalgamated and mud caps are usually absent.

Grain-size grading is generally absent, or poorly developed as a coarse-tail grading with some small pebbles or granules dispersed in a thin basal layer. Beds where the grading is limited to the bed-tops only (top grading) also occur. However, these features are difficult to discriminate since bed boundaries are affected by carbonate redistribution during diagenetic overprint. Probably, compositional grading occurs as a result of the variable bulk density of the bioclastic carbonate grains. Also, stratification and lamination are essentially absent, although a faint parallel lamination is indicated in some rare cases. Generally, beds appear massive and structureless.

Interpretation. The facies represents exclusively T_a divisions of the Bouma sequence or S_3 divisions of the Lowe sequence and corresponds to facies B1.1 of Pickering et al. (1989).

Transport process

Although clear vertical trends are missing, sediment grade and thickness point to transport by hyperconcentrated or concentrated density flows (Mulder and

Alexander 2001). Such flows were previously called sandy debris flows by Shanmugam (1996, 1997, 2000).

Depositional process

Thick/medium-bedded, disorganized sands arise from rapid mass deposition due to intergranular friction in a concentrated dispersion near the bed (Lowe 1982; Pickering et al. 1989). The resultant open-grain packing may have collapsed during or after deposition of the entire bed.

Grainstone/packstones, organized (C2.1/C2.2)

Description. This facies comprises mostly coarse to medium lime sand beds that typically show a relatively well-developed normal grading, lamination and locally cross-lamination. The facies consists of medium to thick beds that usually lack mud caps. Scours and amalgamation rarely occur (Fig. 4A).

Grading and/or lamination are the characteristic internal sedimentary structures displaying base-dominated Bouma sequences, although the Bouma sequences are never complete. Distribution grading predominates, but many beds show coarse-tail grading in their lower parts and distribution grading in their upper parts. The bed grain-size ranges from medium/coarse to granule lime sand at the base, locally with small pebbles along the basal surface, to fine/medium lime sand at the top. This general trend is modified by multilayering and outsized clasts resulting from the calcareous clast composition. In particular, inverse grading as a consequence both of different effective density and different hydraulic behaviour between lithoclasts and various biodetritus (see Eberli 1991; Einsele 1991) is common, above all at the base of some beds but also higher up within individual laminae. In addition, poor sorting results from polymodal composition (including cortoids, peloids and diverse biodetrital grains). A typical normally graded bed displays the following trend of depositional textures:

Top:

- Cortoid/peloid grainstones-packstones (Ø =0.05–0.2 mm, mostly 0.1 mm) well sorted
- Cortoid grainstones (Ø =0.05–0.2 mm, mostly 0.1 mm) well sorted
- Bioclastic grainstones (Ø =0.05–0.5 mm) poorly sorted
- Crinoid grainstones (Ø =0.5–1.5 mm)
- Cortoid grainstones (Ø =0.1–0.4 mm, mostly 0.2 mm) well sorted

Base:

- Lithoclastic packstones to rudstones (Ø =0.5–4 mm, granule lithoclasts)

In some cases diagenetic underbeds mimic a basal micritic layer. Roundness and sphericity of carbonate particles are highly variable, changing rapidly from laminae to laminae and from grain-type to grain-type. Within packstones the morphometric criteria are commonly obliterated by pressure dissolution. A high percentage of plate-like bioclasts and lithoclasts are oriented parallel to lamination.

Interpretation. Most beds representing this facies can be principally described using the Bouma (1962) sequence for classic turbidites. Structural and textural differences mainly result from the calcareous composition (see Meischner 1964; Eberli 1991; Einsele 1991). The facies corresponds to facies C2.1 and C2.2 of Pickering et al. (1989), although mud caps are usually missing. Carbonate mud does not develop surface electrostatic charges which would lead to flocculation, as with siliciclastic clay minerals. Hence, the muddy part of calcareous turbidites could be easily redispersed into the water column with the subsequent following turbidity current (Eberli 1991). A second possible process could be flow splitting (Heath and Mullins 1984; Masson 1994)

Transport process. The progressive changes in grain-size and sedimentary structures indicate transport by concentrated density flows which were transformed into turbidity flows by fluid entrainment and dilution as the flow travelled (Mulder and Alexander 2001). The proportion of the flows in which grain-to-grain interaction dominated decreased, whereas the proportion of the flows in which fluid turbulence was the more important particle-support mechanism increased.

Depositional process. According to the model of Stow and Bowen (1980) the predominant depositional process was grain-by-grain deposition from suspension, followed either by burial (T_a) or by traction transport as bed load ($T_{b,c}$). Progressive transformation from concentrated density flows into turbidity flows tends to improve grading and decreases the thickness of the T_a division.

Grainstone–wackestone couplets, graded-laminated (C2.2/C2.3)

Description. This facies is generally made of bipartite beds that comprise a lower sandy division (grainstone/packstone) and an upper muddy division. The latter comprise lime mud below (wackestone) and commonly siliciclastic mud above (shale). Overall grading and parallel lamination are common internal structures. The medium to thin beds have a sand/mud thickness ratio >1. Tool marks are common sole markings. The base of beds rarely show deep scour structures, but usually are smooth and planar. The tops of beds are generally smooth to planar since the upper part of the bed contains substantial amounts of mud. Bioturbation commonly occurs within thin beds and is restricted to the tops of the beds.

Beds tend to show overall normal grading and/or parallel lamination, and the Bouma sequence is never com-

plete and not readily applicable. Top-cut-out sequences are most typical ($T_{a,b}$ $T_{a,b,c}$), but base-cut-out sequences occur as well ($T_{b,c,d,e}$ $T_{c,d,e}$ $T_{d,e}$). Further possible internal sedimentary structures are basal layers of granule-sized grains, graded lamination, inverse to normal overall grading, faint parallel lamination, rare faint cross lamination and outsized clasts. The bed grain-size ranges from medium/coarse to granule lime sand at the base to lime mud (bimodal sorted bioclastic wackestone) at the top. An ideal inverse to normal graded sequence displays the following depositional textures:

Top:

- Bioclastic wackestone (bimodal sorted)
- Cortoid/peloid packstone (Ø =0.05–0.2 mm, mostly 0.1 mm)
- Cortoid grainstones (Ø =0.05–0.2 mm, mostly 0.1 mm) well sorted
- Bioclastic grainstones (Ø =0.05–0.5 mm) poorly sorted
- Crinoid grainstones (Ø =0.5–1.5 mm)

Base:

- Cortoid grainstones (Ø =0.05–0.2 mm, mostly 0.1 mm) well sorted

Interpretation. Many beds representing this facies can be principally described using the Bouma (1962) sequence for classic turbidites or the Meischner (1964) sequence for allodapic limestones (see the section above on grainstone/packstones, organized). The facies corresponds to facies C2.2 and C2.3 of Pickering et al. (1989). Mud caps are commonly preserved since siliciclastic mud, which represent the hemipelagic background sedimentation, protects the carbonate mud from redispersion.

Transport process
: The Bouma sequences were produced by subcritical and depletive, surge-like turbidity flows (see Mulder and Alexander 2001). Beyond a hydraulic jump as proposed by Morris et al. (1998), the flow has a lower velocity and its sediment load is mostly fine grained (fine sand and finer) and fully transported in suspension.

Depositional process
: The pebbly layers at the base (T_a) probably formed during passage of the erosive flow head, whereas the upper part of the deposits ($T_{b\text{-}d}$) was deposited by the tail of the flow with subsequent traction transport. The depletive flows tend to produce progressive changes in sedimentary structures and grain-size: Parallel lamination T_b corresponding to the upper flow regime, cross-lamination T_c and parallel-lamination T_d corresponding to the lower flow regime, draped by fine sediments T_e. Non-uniform distribution of grain-size can explain the lack of individual divisions of the Bouma sequences.

Packstone-wackestone couplets, graded-laminated (C2.3/D2.1)

Description. This facies generally consists of thin to very thin limestone beds that are interbedded with shale. Soles are mostly sharp whereas bed tops tend to be gradational. The limestone beds are mostly composed of packstones grading upward into calcisiltites that do not have bimodal composition. Normal overall distribution grading prevails. In other cases the beds are homogeneous or thoroughly laminated. The Bouma sequence is usually not applicable. The morphometric criteria are commonly obliterated by pressure dissolution. A high percentage of elongate bioclasts are oriented parallel to lamination.

Interpretation. This facies is roughly comparable with facies C2.3 and D2.1 of Pickering et al. (1989). Internal sedimentary structures, such as overall grading, faint parallel lamination and poor sorting, are typical features that result from the calcareous composition (see Eberli 1991).

Transport process
: Thickness, sediment grade and progressive change in grain-size indicate transport by depletive turbidity flows at the lower end of the concentration range (see Mulder and Alexander 2001).

Depositional process
: According to Stow and Bowen (1980) the principal depositional process is grain-by-grain deposition from suspension, sometimes followed by traction transport along the bottom producing lamination.

Provenance

The **composition of limestone clasts** clearly reflects a reef source for a great number of the subaqueous density-flow deposits studied in the Tiflet section (see Table 2). The primary source area is best interpreted as a reef-rimmed carbonate platform. The photozoan benthic particle association indicates warm tropical conditions during the Givetian within associated shallow-water environments.

Redeposition from reef, reef talus, or peri-reefal deposits is indicated by gravel-sized lithoclasts of already lithified bioclastic sands, and by colonial organisms as well as smaller bioclasts. Archetypal organisms of Middle Devonian reefs and reef mounds are stromatoporoids, colonial tabulate and rugosan corals and solenoporacean calcareous algae (e.g. Birenheide 1985; Gosselin et al. 1989; Meyer 1989; Kreutzer 1990; Weller 1991; Machel and Hunter 1994; Whalen et al. 2000a; Copper 2002) whose fragments all occur in the form of redeposited material (Fig. 6D). Resedimented individual blocks of heliolitid coral colonies reach medium boulder size (0.6 m). Lithoclastic and bioclastic gravels vary from angular to rounded depending on the degree of early lithification, original shape and pre-transport history. The

Table 2 Gravel- and sand-sized carbonate particles of Givetian density-flow deposits from Tiflet

Particles	Types	Features
bioclasts	corals	Numerous genera of colonial tabulate corals predominate, above all heliolitid and thamnoporid corals; colonial and solitary rugosans are subordinate; larger fragments include common examples of geopetal fabrics due to reoriented internal sediments
	stromatoporoids	mainly actinostromids ?
	solenoporaceans	rarely preserved
	echinoderms/crinoids	showing large borings and/or micritized rims
	bryozoans	occur rarely, commonly coated by micrite envelopes due to micritization by boring micro-organisms
	brachiopods	usually punctate forms with thick shells; larger bioclasts commonly coated by micrite envelopes due to micritization by boring micro-organisms
	styliolinids, tentaculitids	
	ostracods	
	muellerisphaerids	
	parathuramminid foraminifers	
	trilobites	
	calcispheres	
	mollusk filaments	
cortoids		
peloids		
lithoclasts	cortoid grainstones	consist of cortoids, peloids and more rarely crinoids
	bioclastic rudstones	consist of corals, stromatoporoids, echinoderms, bryozoans, brachiopods, muellerisphaerids and mollusk filaments
	bioclastic grainstones	consist of echinoderms, bryozoans, brachiopods, corals, stromatoporoids, muellerisphaerids and mollusk filaments
	bioclastic grainstones	includes rare superficial ooids
	bioclastic wackestones, densely packed	crinoids, bryozoans, styliolinids, mollusk filaments
	bryozoan wackestones	fragments of bryozoans, sponge spicules, parathuramminid foraminifers, styliolinids
	bioclastic wackestones, sparse packed	styliolinids, mollusk filaments
	peloid grainstones	occur rarely
	mudstones	

primary origin of this material is interpreted as a fore-reef talus deposit of a shallow-water reef actively growing within the upper photic zone.

A substantial proportion of the gravitationally resedimented material obviously comes from sand bars or from the interior of a peritidal carbonate platform. Above all, density-flow deposits showing a grain-size of coarse sand to fine pebble are rich in crinoids, thick-shelled brachiopods and bryozoans which, in many cases, show micritized rims (Fig. 5A,B). Such micritized bioclasts are typically found in flanking beds of Devonian reefs and reef mounds (e.g. Meyer 1989; Kreutzer 1990) and within associated settings of peritidal carbonate platforms. Smaller bio- and lithoclasts with relatively thick destructive micrite envelopes, in which the nature of the primary grain is no longer discernable with certainty, are classified as cortoids (Bathurst 1971; Flügel 1982). These particles contribute over 50% of grains in many of the sand-sized beds (Fig. 5A,B). The boring activity of micro-endolithic organisms such as cyanobacteria, chlorophytes, rhodophytes and fungi (Golubic et al. 1975) represents an important process responsible for the formation of destructive micrite envelopes (Bathurst 1966). Micro-borers attack skeletal carbonate by a process of biochemical dissolution creating intricate networks of fine borings (Hutchings 1986; Ehrlich 1990). Warm sea-water supersaturated with respect to calcium carbonate favours a filling of the borings by micritic cement (Swinchatt 1969; Gunatilaka 1976). Although bioclasts with micrite rims were also described from deeper-water depositional environments (Zeff and Perkins 1979; Hook et al. 1984), cortoids are mostly produced in the photic zone and reach only rock-forming quantities in shallow-water environments (Günther 1990; Perry 1998). The high proportion of cortoids within the density-flow deposits argues for sediment originating from moderate energy locations along the platform margin or shallow lagoons of a more articulated margin. Open, leeward margins are prone to such a situation (Hine 1983). A well-documented modern example is the western slope of the Great Bahama Bank (Eberli et al. 1997; Westphal 1998; Bernet et al. 2000).

Slope-derived material includes a variety of bioclasts and lithoclasts which display a biotic assemblage of styliolinids, tentaculinids, ostracods, fenestellid bryozoans, trilobites, muellerisphaerids, parathuramminid foraminifers, calcispheres and mollusc filaments (Fig. 5C). Such bioclasts usually lack micritized rims. They are typical of lithoclasts with matrix-supported textures and represent a subordinate bioclastic proportion (max. 20%) within the uppermost divisions of sand-sized tur-

bidite beds (T_{c-e}). The lower divisions (T_{a-c}), which are usually rich in shallow-water material, include minor amounts of these assemblages too (<5%). They are evidence for a second source of material. Within Devonian depositional environments, they are typical of autochthonous carbonate accumulations in shelf lagoons with open circulation, along slopes of peritidal platforms, on pelagic platforms (swells) and within adjacent basins. The depositional settings that delivered biodetritus to the studied density-flow deposits were periplatform settings rather than isolated swells, as indicated by the general co-occurrence of reef-derived faunal elements within individual turbidite beds (Fig. 6A). An equivalent pelagic fauna is, of course, also part of the perennial background sedimentation.

Consequently, the majority of **lithoclasts** consisting of bioclastic wackestones, bryozoan wackestones and mudstones are interpreted as extraclasts reworked from periplatform carbonates at upper slope settings (Fig. 6C). By way of contrast, the depositional texture and composition of cortoid grainstone, bioclastic rudstone and most of the bioclastic grainstone lithoclasts indicate an intrabasinal origin. These intraclasts arose from reworking and down-flow redeposition by density flows at the base of slope. Lithoclasts made of bioclastic grainstones with corals, stromatoporoids or rare superficial ooids indicate platform-margin sources (extraclasts).

In general, the component assemblage comprising shallow-water as well as slope elements indicate a deeper platform margin to slope setting for the generation of the density-flow deposits.

Discussion

Calcareous clast composition

Sedimentary structures produced by density flows with high sediment concentration (>50%) and a coarse-grained load (facies class A of Pickering et al. 1989) are more or less the same for both calcareous and siliciclastic deposits, suggesting that in concentrated and hyperconcentrated density flows the influence of compositional difference decreases (Eberli 1991). Water-escape structures, which are common in siliciclastic counterparts (Lowe 1982), have rarely been described in calcareous deposits. Instead, deposits of turbidity flows loaded with calcareous sand and silt commonly (but not always) display sedimentary structures such as inverse grading, faint cross lamination, outsized clasts and other characteristics that differ from the Bouma sequence as a point of reference. Therefore the facies assignment to facies classes B and C of Pickering et al. (1989), which are defined for clastic density-flow deposits, is much more difficult and in many cases ambiguous. Various reasons and details have been discussed by Colacicchi and Baldanza (1986), Eberli (1991) and Einsele (1991).

Transporting density flows

The calcareous detritus of the studied Givetian sequence was mainly transported by concentrated density flows and more rarely by hyperconcentrated density flows into the basin. A key feature is the facies association of cobble rudstones, organized pebbly grainstones/packstones, amalgamated disorganized grainstones/packstones and organized grainstones/packstones (see the various subsections in the Section - Facies of sediment-flow deposits). Boulder rudstones, such as the major beds exposed at profile-metres 26.90–30.50, reach 1.7 m in thickness and include a maximum clast size of 0.6 m. This association records rare erosional events associated with concentrated density flows which may attain high velocities. Surges were probably common during the early stages of flow and gave rise to repetitions of grading, amalgamated beds and internal erosion surfaces. The absence of mudstone caps and the low amount of autochthonous background sediment within the lower part of the sequence points to a high rate of recurrence of sediment density-flow events.

Organized grainstone to wackestone couplets (see above) interbedded with hemipelagic siliciclastics are exposed preferentially in the upper part of the succession. Overall grading and parallel lamination are common features. A faint cross lamination rarely occurs. Bed thickness ranges from less than 1 cm up to 25 cm. This association was deposited from turbidity flows loaded with fine-grained calcareous sand and silt at times of reduced lime gravel and sand supply to the basin.

Carbonate apron setting

Slope sediments accumulate in extensive, basinwards-thinning wedges which appear to be generated mostly during relative sea-level highstands (Glaser and Droxler 1991; Schlager et al. 1994). The detritus of peritidal carbonate platforms may be carried into the basin by submarine canyons, but commonly there are a series of small gullies cutting the slope, fed from various sources along the margin rather than a single point source. These

Fig. 4 Component assemblage from toe-of-slope deposits at a reef-rimmed platform: Givetian of the Rabat-Tiflet-Zone in Morocco. Photomicrographs of thin sections oriented perpendicular to bedding in plane polarized light. **A** A rare example of scour and fill at the base of an arenitic turbidity flow deposit (facies C2.2). The erosive contact is locally modified by pressure dissolution. The granule-sized fill is made of crinoid, brachiopod, stromatoporoid, coral and bryozoan debris. Sample T-03, Tiflet at 5.55 m. Scale bar is 1 cm. **B** Rudstone forming the base of a concentrated density-flow deposit (facies A2.8). A well defined normal distribution-grading is evident along the left hand margin of the figure. The very coarse lithoclastic pebble exhibit a stromatoporoid overgrown by a heliolitid coral. Medium to fine pebbles comprise stromatoporoids, thamnoporid corals, crinoids, bryozoans and lithoclasts (nearly always bioclastic grainstones). The packstone above mainly consists of peloids and cortoids (>70%). Thamnoporid coral settled out of place from the flow. Sample T-10, Tiflet at 16.90 m. Scale bar is 1 cm


A
B

gullies channel the detritus into a series of ephemeral, overlapping, and coalescing lobes rather than single large submarine fans. Carbonate sediment density flows typically contain less mud than siliciclastic flows and therefore do not pass through so far out onto the basin plain, but tend to terminate rather abruptly at the foot of the slope. Based on these and other differences with siliciclastic slopes, Mullins and Cook (1986) and Colacicchi and Baldanza (1986) developed carbonate-apron models for carbonate-slope deposits which have been extensively reviewed (e.g. Tucker 1990; Coniglio and Dix 1992). A genetic approach to classify carbonate margins was presented by Pomar (2001). Facies distribution and toe-of-slope geometries along carbonate platform margins were described by Bosellini (1984), Kenter and Champbell (1991), Stafleu and Schlager (1995), Blomeier and Reijmer (2002) and recently by Whalen et al. (2002a) for a Devonian system.

Based on field studies, sediment gravity-flow models for carbonate breccias and conglomerates have been proposed early by Krause and Oldershaw (1979) and Eberli (1987). Equivalent deposits have been also described from modern basinal sediments in the surrounding of the Bahama platforms, for which the palaeotopographic situation is well known (Crevello and Schlager 1980; Mullins 1983). Indeed, the modern deposits clearly display a higher proportion of mud and in parts mud-supported textures. The rubble is arranged spatially such that disorganized beds are commonly most proximal and graded to graded-stratified beds are most distal. But, one of the main differences between these models is the suggested spatial position of the inversely graded breccias and conglomerates. Generally, these deposits exemplify bipartition of subaqueous sedimentary density flows that show a flow behaviour transitional between cohesive and non-cohesive (frictional flows) as suggested by Ravenne and Beghin (1983) and Norem et al. (1990). The component layers have different dominant sediment-support mechanisms and may finally decouple (Piper and Normark 1983; Masson 1994).

An interpretation of the specific depositional setting is intricate since the spatial distribution of facies types in facies tracts also records a different degree of flow efficiency (Mutti 1992; Richards et al. 1998). The concept of flow efficiency depicts the ability of a flow to carry its sediment load basinwards and to segregate its grain populations into distinct facies types with distance (Mutti et al. 1999). Very highly efficient flows can fully segregate the grain populations contained within the parental flow with distance, thus producing relatively well-sorted facies types and well-separated facies tracts. Conversely, very poorly efficient flows will only partly segregate their different grain populations, thus producing a more limited number of facies types characterized by poor textural sorting. Calcareous density flows are usually surge-like flows and therefore poorly efficient since they are generated by failure of limited volumes of sediment at a platform slope or short-lived storms surges. Typically, the distal and finer-grained deposits of these flows are poorly developed and traction-plus-fallout structures are rare because of high rates of flow deceleration.

With modern carbonate platforms, the downslope transition from mud- to grain-supported textures of density-flow deposits is similar to that described from ancient examples (Mullins et al. 1984; Grammer et al. 1993). The distinction of cohesive and non-cohesive density flows as well as the recognition of their deposits in modern and ancient environments is a much debated subject. Here the classification of Mulder and Alexander (2001) is used. The presence of connected voids between grains enables hyperconcentrated density flows to ingest water, expand and so transform into concentrated density flows or even turbidity flows or both (Hampton 1972; Fisher 1983; Kneller and Buckee 2000; Mulder and Alexander 2001). At the top of the flows, entrainment and the development of a mixing cloud leads to a region with low sediment concentration and to the formation of overriding turbidity flows. As a consequence, proximal density-flow deposits are typically thick with mud-supported fabric, whereas distal deposits are thinner and grain-supported, commonly topped by an organized turbidite bed (e.g. Ineson and Surlyk 1995; Mutti et al. 1999; Blomeier and Reijmer 2002; Scheibner et al. 2003). However hyperconcentrated density flows may also be triggered by liquefaction and other processes without cohesive precursor flows (Mulder and Alexander 2001) and in that case occupy proximal parts of a slope apron. Moreover, the grade of internal bed organisation dues not shows a simple relationship with proximality in every case (Surlyk 1984, 1995; Pickering et al. 1989; Shanmugam 2000).

Gravel-rich density-flow deposits are usually distributed in proximal parts of a carbonate apron (Cook 1983; Harris 1994; Melim and Scholle 1995; Whalen et al. 2000b; Drzewiecki and Simó 2002). Exceptions are thin gravely density-flow deposits which can be commonly traced far into the basin plain (e.g. Crevello and Schlager 1980; Cook and Mullins 1983). Arenitic density-flow deposits that include granules to medium pebbles occur from proximal slope to distal basin settings (>100 km). Topographic irregularities on the slope also play an important

Fig. 5 Component assemblage from toe-of-slope deposits at a reef-rimmed platform: Givetian of the Rabat-Tiflet-Zone in Morocco. Photomicrographs of thin sections oriented perpendicular to bedding in plane polarized light. **A** Bioclastic grainstone from a turbidity flow deposit (facies C2.2). Lime sand comprise cortoids, peloids, brachiopods and crinoids. The two larger grains are a crinoid ossicle (*left*) and a bryozoan fragment (*right*) with thick micritized rims. Sample T-03, Tiflet at 5.55 m. Scale bar is 500 μm. **B** Cortoid grainstone from a turbidity flow deposit (facies C2.2). Thick micritized rims occur on more than 50% of the bioclasts. Sample T-04, Tiflet at 5.63 m. Scale bar is 500 μm. **C** Pebble rudstone from middle part of a concentrated density-flow deposit (facies A2.3) showing normal grading. Lithoclastic debris include grain-supported textures (cortoid grainstones, bioclastic grainstones) as well as mud-supported textures such as styliolinid wackestones (*below centre left*). Bioclastic debris is dominated by crinoids, brachiopods, thamnoporid corals (*centre*), bryozoans and stromatoporoids. Sample T-09, Tiflet at 15.95 m. Scale bar is 1 cm

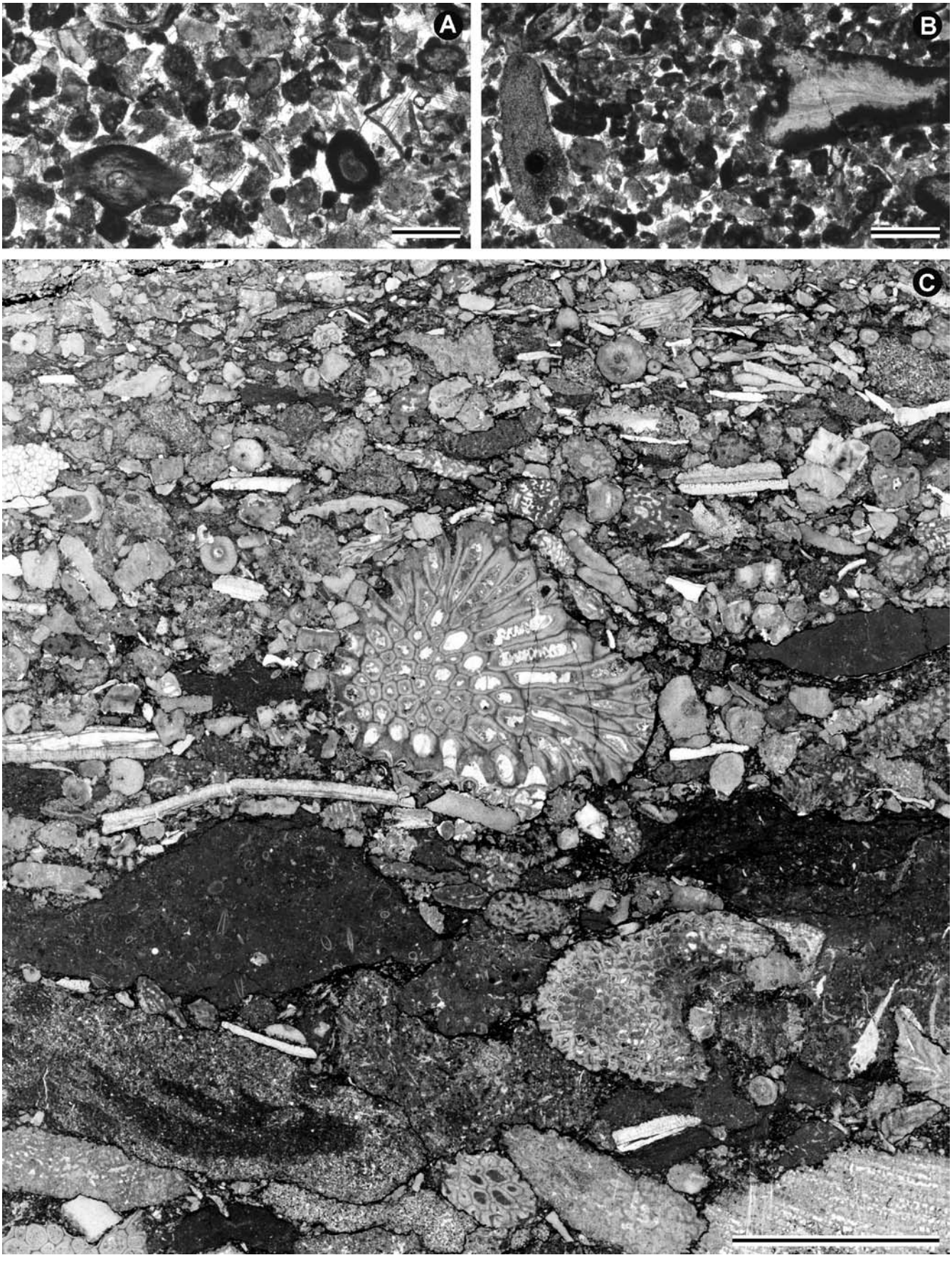
A
B
C

role in controlling the lateral distance that density flows can travel in a basin (Prather et al. 1999).

The facies association and element geometry described here probably represent an outer base-of-slope apron. In modern carbonate aprons of the Bahama platform, the association of coarse-grained (<1 m thick) and finer-grained density-flow deposits (0.2–0.3 m), grain-supported debris-flow deposits and two-layer deposits is found in a distal zone of the lower-slope apron facies (Mullins et al. 1984). Schlager and Chermak (1979) and Crevello and Schlager (1980) consider such sediment wedges of redeposited carbonates at the toe-of-slope as deposits of the basin-margin rise rather than the lower slope. Regardless of this terminological question, the distal apron facies is comparable with the studied facies association of density-flow deposits from Tiflet.

Features indicative of proximal lower slope or upper slope are not evident: Synsedimentary folds formed by slump or creep, low-angle truncation surfaces (slump scars), erosional channels filled with discontinuous layers of sand and rubble, and mud-supported debris-flow deposits. Geopetal internal sediments in primary voids, which would show that enclosing bedding was deposited at an angle to horizontal, are not found. Consequently, the studied sediments represent fore-reef toe-of-slope deposits which were accumulated seaward of the limit of appreciable slope.

The subordinate amount of peri-platform ooze within the succession of Tiflet may have various reasons. It could be also indicative of outer apron sediments (e.g. Mullins et al. 1984), but is likely a result of high input rates of sediment density flows (e.g. Schlager and Chermak 1979), or may reflect the small size of the source platform (e.g. Harris 1994). In addition, the high amount of biologically induced micrites by benthic and planktic biota in modern carbonate environments is not characteristic for Palaeozoic systems.

The carbonate density-flow deposits at Tiflet contain both margin- and slope-derived reworked sediment. Such a mixed composition is indicative for bypass slopes which typically have either a steep slope angle or an erosional scarp (Haas 1999; Drzewiecki and Simó 2002). The occurrence of hyperconcentrated and concentrated density flows loaded with lime gravel and coarse sand also point to a steep escarpment or slope. Fast growing reefs at the platform margin (not mounds) or an active fault may have caused such a steep slope. The driving force of hyperconcentrated density flows is mostly related to gravity. Although run-out distance depends on many factors, such flows cannot be maintained on very-low-angle slopes for as long as more dilute flows (Mulder and Alexander 2001). In concentrated density flows, sediment erosion may be able to maintain the flow even at lower slope gradients and may generate long run-out distances. According to Colacicchi and Baldanza (1986) carbonate turbidity flows are always heavily loaded (due to the low primary amounts of mud), have a very high internal friction (caused by the calcareous mud composition), and are thus subjected to a loss of kinetic energy more rapid than that lost by the well-lubricated clayey turbidity currents. Consequently, carbonate turbidity flows need steep slopes in order to balance the rapid loss of kinetic energy.

Conclusions

The marine record preserved within the Rabat-Tiflet-Zone of Morocco, which is thought to be an equivalent of the Prague Basin of Central Europe, includes a Givetian succession of subaqueous density-flow deposits interbedded with hemipelagic and pelagic muds. They carry a wide range of information about the bathymetry and ecology of the source area as well as the basin-margin setting:

1. The conodont fauna indicates reworking and redeposition of contemporaneous shallow-marine carbonates during the *hemiansatus* and *timorensis* Zones.
2. Calcareous debris was mostly transported by surge-like concentrated density flows and turbidity flows, though hyperconcentrated density flows contributed thick lime gravel beds.
3. Although the uppermost part of the succession displays a thinning and fining upward sequence, sequential organisation of the succession seems to be low.
4. The component assemblage exhibits a photozoan benthic particle association in the neritic source environment.
5. The density-flow deposits are dominated by material sourced from photic environments as well as high-energy shoals of a peritidal carbonate platform. Lime conglomerate beds are particularly rich in coral and stromatoporoid gravel shed from reef, reef talus, or peri-reefal deposits. Arenitic beds mainly comprise cortoids and less intensive micritized bioclasts such as bryozoans, crinoids and thick-shelled brachiopods which are interpreted as constituents initially derived from platform-margin sand shoals or from low-energy lagoons.

Fig. 6 Component assemblage from toe-of-slope deposits at a reef-rimmed platform: Givetian of the Rabat-Tiflet-Zone in Morocco. Photomicrographs of thin sections oriented perpendicular to bedding in plane polarized light. **A** Bioclastic grainstone from the base a turbidity flow deposit (facies C2.3). Crinoid ossicles, ostracod shells and styliolinids are common. Cortoids and peloids predominate within the upper part of the bed. Sample T-05, Tiflet at 8.12 m. Scale bar is 500 µm. **B** Bioclastic grainstone form upper part of a turbidity flow deposit (facies C2.2). Crinoids and brachiopods occur among distinctly smaller peloids and cortoids. Sample T-04, Tiflet at 5.63 m. Scale bar is 500 µm. **C** Lithoclast of a concentrated density-flow deposit (facies A2.3). The bioclastic wackestones include material of shallow-water origin (heavily bored crinoid ossicle) as well as remains of nektic and planktic biogens (styliolinids). Sample T-09, Tiflet at 15.95 m. Scale bar is 500 µm. **D** Rudstone from the lower part of a concentrated density-flow deposit (facies A2.3). Clasts show a dissolution enhanced fitted fabric. Lithoclastic gravel include cortoid grainstones (*lower left and right*) and bioclastic wackestones (*centre and upper part*). Bioclastic gravel is dominated by different genera of thamnoporid corals and stromatoporoids. Sample T-08, Tiflet at 15.82 m. Scale bar is 1 cm

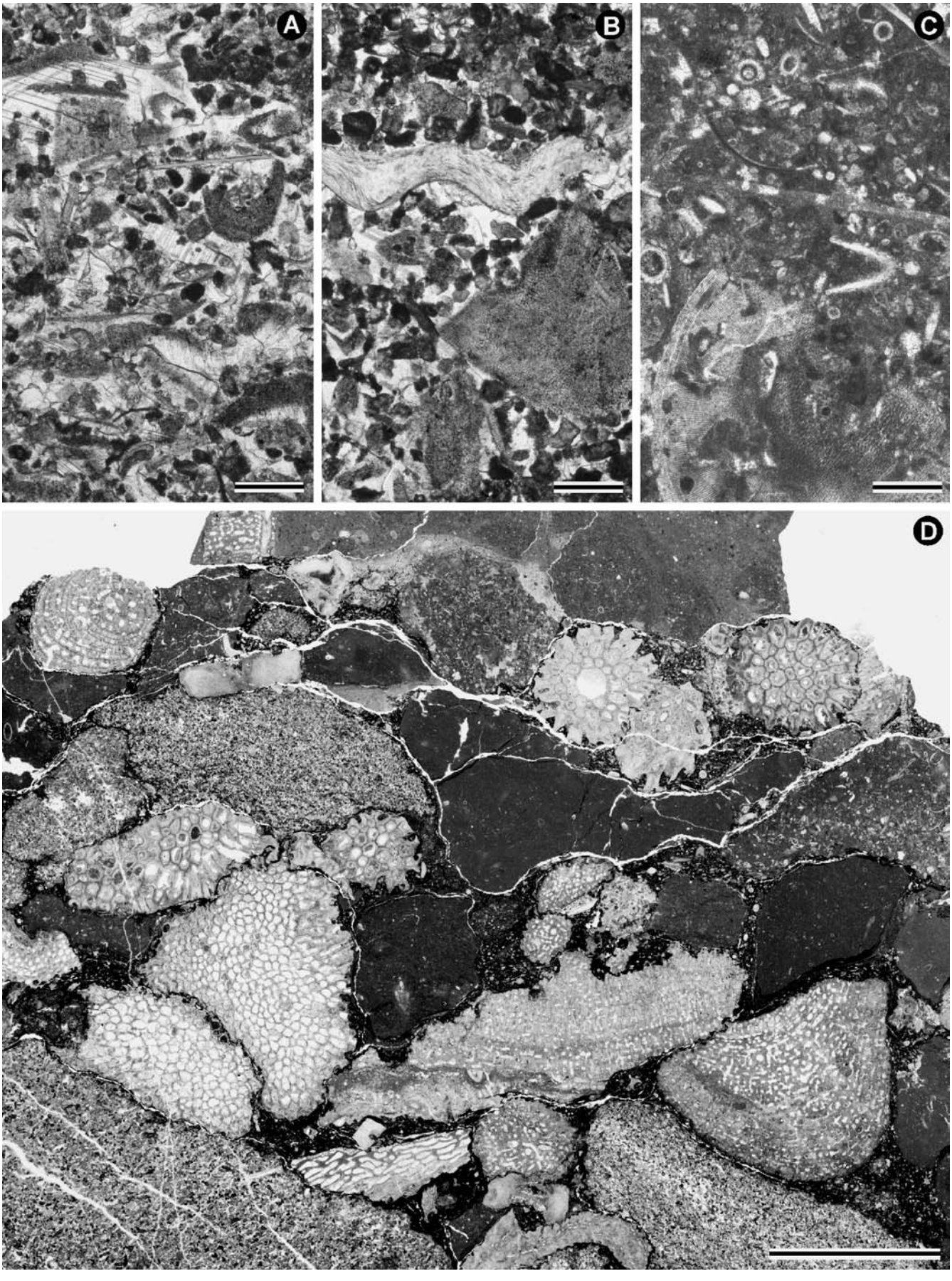
A
B
C
D

6. Periplatform carbonates from upper slope settings were a second source of material which is mainly documented by lithoclasts of mud-supported textures. Typical for periplatform deposits, the shallow-water derived constituents occur together with shells of planktonic organisms such as the Devonian tentaculitids, styliolinids and parathuramminid foraminifers.
7. Density-flow deposits were shed from deeper platform margin to upper slope settings, since most of the beds comprise both constituents of platform-margin gravel and sand as well as of periplatform suspension deposits.
8. The presence of actual reef debris is critical for identifying a fore-reef toe-of-slope setting.
9. The occurrence of hyperconcentrated and concentrated density flows loaded with lime gravel and sand point to a steep slope or escarpment. Fast growing reefs at platform margin or an active basin-bounding fault may have been caused such a steep slope. But so far, there is no indication for erosion at an escarpment by stratigraphic admixtures of older conodont faunas.

Component assemblages are shown in Figs. 4, 5 and 6.

Acknowledgements The facial characterization of the Givetian succession at Tiflet was part of a project in which autochthonous and allochthonous structural units of Moroccan Central Massif were compared. The German Research Foundation (DFG) founded the project and made equipment available for field work in Morocco (Hu 804/1–1). We are particularly grateful to G.K.B. Alberti (University Hamburg), O.H. Walliser (University Göttingen) and T. Becker (University Münster) for supporting our preparations for field work. We are indebted to A. El Hassani (Institut Scientifique, Rabat) for scientific cooperation and logistic support and M. Boutaleb (Ministère de d'Energie et des Mines, Rabat) for issuing a working permit in Morocco. Special thanks are given to H. Weller (University Greifswald) for his helpful introduction to Devonian reef biota, and to S. Foley (University Mainz) for improving the English language of our manuscript. The critical reviews of an early version of the manuscript by M. Tucker (University Durham) and J. Martín-Chivelet (University Madrid) are gratefully appreciated and acknowledged. A. Freiwald and W. Buggisch (University Erlangen) are thanked for their constructive reviews.

References

Alberti GKB (1969) Trilobiten des jüngeren Siluriums sowie des Unter- und Mitteldevons. I. Mit Beiträgen zur Silur-Devon-Stratigraphie einiger Gebiete Marokkos und Oberfrankens. Abh Senckenberg naturforsch Ges 520:1-692

Alberti GKB (1970) Trilobiten des jüngeren Siluriums sowie des Unter- und Mitteldevons. II. Abh Senckenberg naturforsch Ges 525:1-233

Bathurst RGC (1966) Boring algae, micrite envelopes and lithification of molluscan biosparites. Jour Geol 5:15–32

Bathurst RGC (1971) Carbonate sediments and their diagenesis. Elsevier, Amsterdam, 658 pp

Bernet KH, Eberli GP, Gilli A (2000) Turbidite frequency and composition in the distal part of the Bahama transect. In: Swart PK, Eberli GP, Malone MJ, Sarg JF (eds) Proceedings of the Ocean Drilling Program, Scientific Results, 166:45–60. Ocean Drilling Program, College Station, TX

Birenheide R (1985) Chaetetida und tabulate Korallen des Devon. Bornträger, Berlin, 249 pp

Blair TC, McPherson JG (1999) Grain-size and textural classification of coarse sedimentary particles. Jour Sedim Res 69:6-19

Blomeier D, Reijmer JJG (2002) Facies architecture of a Lower Jurassic carbonate platform slope (Jbel Bou Dahar, High Atlas, Morocco). Jour Sedim Res 72:463–476

Bosellini A (1984) Progradation geometries of carbonate platforms: examples from the Triassic of the Dolomites, Italy. Sedimentology 31:1-24

Bouma AH (1962) Sedimentology of some flysch deposits: a graphic approach to facies interpretation. Elsevier, Amsterdam, 168 pp

Bultynck P (1987) Pelagic and neritic conodont succession from the Givetian of pre-Sahara Morocco and the Ardennes. Bull Inst r Sci nat Belg, Sci de la Terre 57:149–181

Chaloupský J, Chlupáč I, Mašek J, Waldhausrová J, Cháb J (1995) Tepla-Barrandian Zone (Bohemicum) Stratigraphy. In: Dallmeyer RD, Franke W, Weber K (eds) Pre-Permian geology of Central and Eastern Europe. Springer, Berlin, pp 379–391

Colacicchi R, Baldanza A (1986) Carbonate turbidites in a Mesozoic pelagic basin: Scaglia Formation, Apennines – comparison with siliciclastic depositional models. Sedim Geol 48:81–105

Coniglio M, Dix GR (1992) Carbonates slopes. In: Walker RG, James NP (eds) Facies models—response to sea-level changes. Geol Assoc of Canada, Memorial Univ St John's, 349–373

Cook HE (1983) Ancient carbonate margins slopes and basins. In: Cook HE, Hine AC, Mullins HT (eds) Platform margin and deepwater carbonates. Soc Econ Paleont Miner, Short Course 12:5.1–5.89

Cook HE, Mullins HT (1983) Basin margin environment. In: Scholle PA, Bebout DG, Moore CH (eds) Carbonate depositional environments. Am Ass petrol Geol Mem 33:540–617

Copper P (2002) Silurian and Devonian reefs: 80 million years of global greenhouse between two ice ages. In: Kiessling W, Flügel E, Golonka J (eds) Phanerozoic reef patterns. Soc Sedim Petrol Spec Publ 72:181–238

Crevello PD, Schlager W (1980) Carbonate debris sheets and turbidites, Exuma Sound, Bahamas. Jour Sedim Petrol 50:1121–1148

Destombes J, Hollard H, Willefert, S (1985) Lower Palaeozoic rocks of Morocco. In: Holland CH (ed) Lower Palaeozoic rocks of the world. John Wiley, London, pp 91–336

Drzewiecki PA, Simó JA (2002) Depositional processes triggering mechanisms and sediment composition of carbonate gravity-flow deposits: examples from the Late Cretaceous of the south-central Pyrenees, Spain. Sedim Geol 146:155–189

Dunham RJ (1962) Classification of carbonate rocks according to depositional texture. In: Ham WE (ed) Classification of carbonate rocks. Amer Assoc petrol Geol Mem 1:108–121

Eberli GP (1987) Carbonate turbidite sequences deposited in rift-basins of the Jurassic Tethys Ocean (eastern Alps, Switzerland). Sedimentology 34:363–388

Eberli GP (1991) Calcareous turbidites and their relationship to sea-level fluctuations and tectonism. In: Einsele G, Ricken W, Seilacher, A (eds) Cycles and events in stratigraphy. Springer, Berlin, pp. 340–359

Eberli GP, Swart PK, McNeill DF, Kenter JAM, Anselmetti FS, Melim LA, Ginsburg RN, (1997) A synopsis of the Bahama drilling project: results from two deep core borings drilled on the Great Bahama Bank. In: Eberli GP, Swart PK, Malone MJ (eds) Proceedings of the Ocean Drilling Program, Initial Reports, 166:23–42, Ocean Drilling Program, College Station, TX

Ehrlich HL (1990) Microbial formation and degradation of carbonates. In: Ehrlich HL (ed) Geomicrobiology. Marcel Dekker, New York, pp. 157–195

Einsele G (1991) Submarine mass flow deposits and turbidites. In: Einsele G, Ricken W, Seilacher A. (eds) Cycles and events in stratigraphy. Springer, Berlin, pp. 313–339

El Hassani A (1991) La zone de Rabat-Tiflet: Bordure nord de la chaîne calédono-hercynienne du Maroc. Bull Inst Sci Rabat 15:1-134

Embry AF, Klovan JE (1972) Absolute water depth limits of Late Devonian palecological zones. Geol Rdsch 61:672–686

Fisher RV (1983) Flow transformations in sediment gravity flows. Geology 11:273–274
Flügel E (1982) Microfacies analysis of limestones. Springer, Berlin, 633 pp
Gee MJR, Masson DG, Watts AB, Allen PA (1999) The Saharan debris flow: an insight into the mechanics of long run-out submarine debris flows. Sedimentology 46:317–335
Ghibaudo G (1992) Subaqueous sediment gravity-flow deposits: practical criteria for their field description and classification. Sedimentology 39:423–454
Glaser KS, Droxler AW (1991) Highstand production and highstand shedding from deeply submerged carbonate banks northern Nicaragua Rise. Jour sedim Petrol 61:128–142
Golubic S, Perkins RD, Lukas KJ (1975) Boring microorganisms and microborings in carbonate substrates. In: Frey RW (ed) The study of trace fossils. Springer, Berlin, pp. 229–259
Gosselin EG, Smith L, Mundy, DJC (1989) The Golden end Evi Reef complexes, Middle Devonian Slave Point Formation, northwestern Alberta. In: Geldsetzer HHJ, James NP, Tebbutt GE (eds) Reefs Canada and adjacent areas. Can Soc Petrol Geol Mem 13:440–447
Grammer GM, Ginsburg RN, Harris PM (1993) Timing of deposition, diagenesis and failure of steep carbonate slopes in response to high-amplitude/high-frequency fluctuation in sea level, Tongue of the Ocean, Bahamas. Am Assoc Petrol Geol Mem 57:107–131
Gunatilaka A (1976) Thallophyte boring and micritization within skeletal sands from Connemara, Western Ireland. Jour Sedim Petrol 46:548–554
Günther A (1990) Distribution and bathymetry zonation of shell-boring endoliths in recent reef and shelf environments: Cozumel Yucatan (Mexico). Facies 22:233–262
Haas J (1999) Genesis of Late Cretaceous toe-of slope breccias in the Bakony Mts, Hungary. Sedim Geol 128:51–66
Hampton MA (1972) The role of subaqueous debris flow in generating turbidity currents. Jour Sedim Petrol 42:775–793
Harris MT (1994) The fore-slope and toe-of-slope facies of the Middle Triassic Latemar Buildup (Dolomites, Northern Italy). Jour Sedim Res 64:132–145
Heath KC, Mullins HT (1984): Open-ocean off-bank transport of fine-grained carbonate sediment in the northern Bahamas. In: Stow DAV, Piper DJW (eds) Fine-grained sediments: deep-water processes and facies. Geol Soc London Spec Publ 15: 199–208
Hine AC (1983) Modern carbonate platform margins. In: Cook HE, Hine AC, Mullins HT (eds) Platform margin and deepwater carbonates. Soc Econ Paleont Miner Short Course 12:3.1–3.96
Hiscott RN (1994) Traction-carpet stratification in turbidites – facts or fiction? Jour Sedim Res A64:204–208
Hiscott RN (1995) Traction-carpet stratification in turbidites – facts or fiction? (reply). Jour Sedim Res A65:704–705
Hollard H (1967) Le Dévonien du Maroc et du Sahara nord-occidental. In: Oswald DH (ed) International Symposium on the Devonian System, Calgary, vol 1. Alberta Soc Petrol Geol, Calgary, pp. 203–244
Hook JE, Golubic S, Milliman JD (1984) Micrite cement in microborings is not necessarily a shallow-water indicator. Jour Sedim Petrol 54:425–431
Hutchings PA (1986) Biological destruction of coral reefs: a review. Coral Reefs 4:239–252
Ineson J, Surlyk F (1995) Carbonate slope aprons in the Cambrian of North Greenland: geometry stratal patterns and facies. In: Pickering KT, Hiscott RN, Kenyon NH, Ricci Lucchi F, Smith RDA (eds) Atlas of deep water environments: architectural style in turbidite systems. Chapman and Hall, London, pp. 56–62
Inverson RM (1997) Physics of debris flows. Rev Geophys 35:245–296
Julien PY, Lan Y (1991) Rheology of hyper-concentrations. Jour Hydraul Eng 117:346–353
Junge P (1997) Stratigraphie (Conodonten) und Sedimentologie der mittel- und oberdevonischen Flinzkalke südlich von Wernigerode (Harz). Ph D Thesis Univ Greifswald FR Geowissenschaften, Greifswald, Germany, 140 pp
Kenter JAM, Champbell AE (1991) Sedimentation on a Jurassic carbonate platform flank: geometry sediment fabric and related depositional structures (Djebel Bou Dahr, High Atlas, Morocco). Sedim Geol 72:1-34
Kneller B, Buckee C (2000) The structure and fluid mechanics of turbidity currents: a review of some recent studies and their geological implications. Sedimentology 47 (Supplement 1): 62–94
Krause F, Oldershaw, AE (1979) Submarine carbonate breccia beds. Can Jour Earth Sci 16:189–199
Krebs W (1964) Zur faziellen Deutung von Conodonten-Mischfaunen Senckenbergiana lethaea 45:245–284
Kreutzer LH (1990) Mikrofazies Stratigraphie und Paläogeographie des Zentralkarnischen Hauptkammes zwischen Seewarte und Cellon. Jahrb Geol Bundesanst Wien 133:275–343
Lowe DR (1982) Sediment gravity flows: II. Depositional models with special reference to the deposits of high-density turbidity currents. Jour Sedim Petrol 52:279–97
Machel HG, Hunter IG (1994) Facies models for Middle to Late Devonian shallow-marine carbonates with comparison to modern reefs: a guide to facies analysis. Facies 30:155–176
Major JJ (1997) Depositional processes in large-scale debris-flow experiments. Jour Geol 105:345–366
Marr J, Harff P, Shanmugam G, Parker G (1997) Experiments on subaqueous sandy debris flows. Supplement to EOS Transactions, AGU Fall Meeting, San Francisco, 78 (46), F347
Masson DG (1994) Late Quaternary turbidite current pathways to the Madeira Abyssal Plain and some constraints on turbidity current mechanisms. Basin Res 6:17–33
Meischner KD (1964) Allodapische Kalke Turbidite in Riff-nahen Sedimentationsbecken. In: Bouma AH, Brouwer A (eds) Turbidites. Elsevier, Amsterdam, pp. 156–191
Melim LA, Scholle PA (1995) The fore-reef facies of the Permian Capitan Formation: the role of sediment supply versus sea-level changes. Jour Sedim Res B65:107–118
Meyer FO (1989) Stromatoporoid-coral patch reefs of Givetian age, Michigan. In: Geldsetzer HHJ, James NP, Tebbutt GE (eds) Reefs, Canada and adjacent areas. Can Soc Petrol Geol Mem 13:492–496
Mohrig D, Whipple KX, Hondzo M, Ellis C, Parker G (1998) Hydroplaning of subaqueous debris flows. Geol Soc Am Bull 110:387–394
Morris SA, Kenyon NH, Limonov AF, Alexander J (1998) Downstream changes of large-scale bedforms in turbidites around the Valancia Channel Mouth, Northwest Mediterranean: implications for palaeoflow reconstruction. Sedimentology 45: 365–377
Mulder T, Alexander J (2001) The physical character of subaqueous sedimentary density flows and their deposits. Sedimentology 48:269–299
Mullins HT (1983) Modern carbonate slopes and basin of the Bahamas. In: Cook HE, Hine AC, Mullins HT (eds) Platform margin and deepwater carbonates. Soc Econ Paleont Miner Short Course 12:4.1–4.138
Mullins HT, Cook HE (1986) Carbonate apron models: alternatives to the submarine fan model for palaeoenvironmental analysis and hydrocarbon exploration. Sedim Geol 48:37–79
Mullins HT, Heath KC, van Buren HM, Newton CR (1984) Anatomy of a modern open ocean carbonate slope: Northern Little Bahama Bank. Sedimentology 31:141–168
Mutti E (1992) Turbidite sandstones. Agip Instituto di Geologia, Università di Parma, San Donato Milanese
Mutti E, Tinterri R, Remacha E, Mavilla N, Angella S, Fava L (1999) An introduction to the analysis of ancient turbidite basins from an outcrop perspective. Am Assoc Petrol Geol Continuing Education Course Note Series 39:1-61
Norem H, Locat J, Schieldrop B (1990): An approach to the physics and the modelling of submarine flow-slides. Mar Geotechnology 9:93–111

Perry CT (1998) Grain susceptibility to the effect of microboring: implications for the Preservation of skeletal carbonates. Sedimentology 45:39–51

Pickering KT, Stow DAV, Watson M, Hiscott RN (1986) Deep-water scheme for modern and ancient sediments. Earth Sci Reviews 22:75–174

Pickering KT, Hiscott RN, Hein FJ (1989) Deep marine environments: clastic sedimentation and tectonics. Unwin Hyman, London, 416 pp

Piper DJW, Normark WR (1983) Turbidite depositional patterns and flow characteristics, Navy Submarine Fan, California Borderland. Sedimentology 30:681–694

Pomar L (2001) Types of carbonate platforms: a genetic approach. Basin Res 13:313–334

Prather BE, Booth JR, Steffens GS, Craig PA (1999) Classification lithologic calibration and stratigraphic succession of seismic facies of inter-slope basins, deep-water Gulf of Mexico. Am Assoc Petrol Geol Bull 82:701–728

Ravenne C, Beghin P (1983) Apport des experiences en canal à l'interprétation sédimentologique des depots de cones détriques sous-marines. Rev Inst Fr Pétrol 38:279–297

Richards M, Bowman M, Reading H (1998) Submarine-fan systems I: characterization and stratigraphic prediction. Mar Petr Geol 15:689–717

Savoye B, Piper DJW, Droz L (1993) Plio-Pleistocene evolution of the Var deep-sea fan off the French Riviera. Mar Petrol Geol 10:550–571

Scheibner C, Reijmer JJG, Marzouk AM, Speijer RP, Kuss J (2003) From platform to basin: the evolution of a Palaeocene carbonate margin (Eastern Dessert, Egypt). Int Jour Earth Sci 92:624–640

Schlager W, Chermak A (1979) Sediment facies of platform-basin transition, Tongue of the Ocean, Bahamas. In: Doyle LJ, Pilkey OH (eds) Geology of continental slopes. Soc Econ Paleont. Miner Spec Publ 27:193–207

Schlager W, Reijmer JJG, Droxler A (1994) Highstand shedding of carbonate platforms. Jour Sedim Res B64:270–281

Shanmugam G (1996) High-density turbidity currents: are they sandy debris flows? Jour Sedim Res 66:2-10

Shanmugam G (1997) The Bouma sequence and the turbidite mind set. Earth-Sci Rev 42:201–229

Shanmugam G (2000) 50 years of turbidite paradigm (1950s-1990 s): deep-water processes and facies models – a critical perspective. Mar Petrol Geol 17:285–342

Sohn TK (1997) On traction-carpet sedimentation. Jour Sedim Res 67:502–509

Stafleu J, Schlager W (1995) Pseudo-unconformities in seismic models of large outcrops. Geol Rundsch 84:761–769

Stow DAV, Bowen AJ (1980) A physical model for the transport and sorting of fine-grained sediments by turbidity currents. Sedimentology 27:31–46

Surlyk F (1984) Fan-delta to submarine fan conglomerates of the Volgian-Valanginian Wollaston Foreland Group, East Greenland. In: Koster EH, Steel RJ (eds) Sedimentology of gravels and conglomerates. Can Soc Petrol Geol Mem 10:359–82

Surlyk F (1995) Deep-sea fan valleys channels lobes and fringes of the Silurian Peary Land Group, North Greenland. In: Pickering KT, Hiscott RN, Kenyon NH, Ricci Lucchi F, Smith RDA (eds) Atlas of deep water environments: architectural style in turbidite systems. Chapman and Hall, London, pp. 124–138

Swinchatt JP (1969) Algal boring: a possible depth indicator in carbonate rocks and sediments. Geol Soc Am Bull 80:1391–1396

Tucker ME (1990) Carbonate depositional systems II: deeper-water facies of pelagic and resedimented limestones. In: Tucker ME, Wright VP (eds) Carbonate sedimentology. Blackwell, Oxford, pp. 228–283

Walliser OH, Bultynck P, Weddige K, Becker RT, House MR (1995a) Definition of the Eifelian–Givetian stage boundary. Episodes 18/3:107–115

Walliser OH, El Hassani A, Tahiri A (1995b) Sur le Dévonien de la Meseta marocaine occidentale: Comparaisons avec le Dévonien allemand et événements globaux. Cour Forsch-Inst Senckenberg 188:21–30

Weddige K (1977) Die Conodonten der Eifel-Stufe im Typusgebiet und in benachbarten Faziesgebieten. Senckenbergiana lethaea 58:271–419

Weller H (1991) Facies and development of the Devonian (Givetian/Frasnian) Elbingerode Reef Complex in the Harz area (Germany). Facies 25:1-50

Westphal H (1998) Carbonate platform slopes – a record of changing conditions: the Pliocene of the Bahamas. Lecture Notes in Earth Sciences 75, Springer, Berlin, 197 pp

Whalen MT, Eberli GP, van Buchem FSP, Mountjoy EP (2000a) Facies architecture of Upper Devonian carbonate platforms, Rocky Mountains, Canada. In. Homewood PW, Eberli GP (eds) Genetic stratigraphy on the exploration and production scales – case studies from the Pennsylvanian of the Paradox Basin and the Upper Devonian of Alberta. Bull Cent Rech Elf Explor-Prod Mem 24:139–178

Whalen MT, Eberli GP, van Buchem FSP, Mountjoy EP, Homewood PW (2000b) Bypass margins, basin-restricted wedges, and platform-to-basin correlation, Upper Devonian, Canadian Rocky Mountains: implications for sequence stratigraphy of carbonate platform systems. Jour Sedim Res 70:913–936

Zeff ML, Perkins RD (1979) Microbial alteration of Bahamian deep sea carbonates. Jour Sedim Petrol 26:175–201

Ziegler W, Klapper G, Johnson JG (1976) Redefinition and subdivision of the *varcus* zone (conodonts, Middle/ ? Upper Devonian) in Europe and North America. Geologica et Palaeontologica 10:109–140